UNIVERSITY OF CALIFORNIA

Los Angeles

Use of Wavelet Transformation to Identify Longitudinal Trends of Time-Frequency Components in Visual Learning Paradigm

Master of Science in Biostatistics

By:

Cameron S. Goldbeck

Advisor:

Damla Senturk

June 3, 2018

Table of Contents

1 Introduction **1**

1.1 Contextual Introduction 1

1.2 Previous Work 1

1.3 Wavelet Transformation 3

2 Data **4**

2.1 Experimental Conditions 4

2.2 Data Structure 5

3 Method **6**

3.1 Outline 6

3.2 Notation 7

3.3 Algorithm 8

4 Analysis and Results **9**

4.1 Implementing Transformation 9

4.2 Results 10

4.3 Findings & Discussion 11

References **14**

List of Figures

1 Visualization of Experiment 16

2 ASD Delta Direction 17

3 ASD Theta Direction 18

4 TD Delta Direction 19

5 TD Theta Direction 20

6 ASD Delta Power 21

7 ASD Delta Time 22

8 ASD Theta Power 23

9 ASD Theta Time 24

10 TD Delta Power 25

11 TD Delta Time 26

12 TD Theta Power 27

13 TD Theta Time 28

Abstract

Cerebral responses to visual stimuli in the form of Electroencephalograms (EEG) and associated Event Related Potentials (ERPs) can provide meaningful insight in a variety of learning paradigms. However, due to the nature in which the data is collected, there is a low signal-to-noise ratio preventing meaningful analysis on the raw data. Previous works have utilized time domain and frequency domain techniques to boost low signal-to-noise but fail to give insight to the nuances of the Time-Frequency relationship. We propose the use of Wavelet Transformations to further understand learning differences and processes between children with Autism Spectrum Disorder and their Typically Developing counterparts. Wavelet Transformation, which have been shown to be effect tools in EEG /ERP analysis, contain high time AND frequency resolution that when combined with Principal Component Analysis lead to results that have a boosted signal-to-noise ratio and demonstrate the relationship Delta and Theta frequency bands have on well know temporal measures.

1 Introduction

1.1 Contextual Introduction

Electroencephalograms (EEG) and associated Event Related Potentials (ERPs) in response to stimuli are common methods of analyses when measuring brain activity that yield very high time resolution in the form of functional data. Due to the low level voltage response from the brain in sensory experiments, usually a few microvolts, raw EEG data typically has a low signal-to-noise ratio (SNR) so in order to compensate for this established issue, single ERPs are typically averaged over repeated trials. However, doing so leads to a loss of longitudinal information regarding the dynamic processes over exposures, which could contain important inference.

1.2 Previous Work

Methods have been created to balance the need to combine ERP trials in order to boost the SNR while also maintaining the longitudinal dimension of the data. In [1], a meta-preprocessing technique in which a moving trial window of 30 is utilized to average all trials in the window for a individual subject, condition, and electrode. By doing so, investigators were able to boost SNR allowing measures of interest, e.g. P300 and N100 amplitudes, to be more reliably measured while also allowing for them to change over trials. However, there are drawbacks with this meta-preprocessing method. Firstly, whenever ERPs are averaged, damping of the signal occurs; this

is when peaks of signals to be averaged are not aligned resulting in the averaged waveform having a smaller, and biased, estimated amplitude. Secondly, this analysis is conducted solely in the time domain, therefore, there is no frequency information regarding the amplitudes, e.g. Delta or Theta band contributions.

Alternative methods have successfully shown the use of frequency domain based smoothing and decompositions of EEG data. In [2], a time-localized Fourier decomposition is applied over locally stationary brain signals before, during, and after a seizure event. In order to obtain consistent estimates of time-localized periodograms, smoothing kernels were applied over frequencies before Principal Component Analysis was applied. By performing analysis completely in the frequency domain, investigators were able to examine influential frequency bands, signal channels, and coherency between channels throughout a seizure event. Similarly to studies performed only in the time domain, however, analysis performed only in the frequency domain lacks any temporal information, e.g. P300 amplitude. Additionally, the waveforms in this study were collected over long exposures, about 2 minutes. When this is not the case, time-localized Fourier decomposition is challenging because exposure may only be a second or two and Fourier decomposition is not suited for very small time segments with few observed points.

Promising methods that have shown to be effective on short ERP waveforms, as well as providing both time and frequency information, are the use of wavelets functions as the basis for decompositions. In [3], a large variety of time-frequency

transformation are examined for the use in EEG and ERP data as well as their benefits over simpler Fourier transforms. Unlike the Fourier Transformation which uses sines and cosines as its basis, Wavelet Transformation use more unique functions such as the Morlet, Symlet, or Meyer wavelets. These basis functions do not posses the global behavior of the trigonometric functions meaning their frequency response is localized in functional time. It is because of this high time AND frequency resolution, they are able to detect concurrent yet distinct activity in different frequency bands and time windows that would otherwise be missed if analyzed in just one of the two domains.

1.3 Wavelet Transformation

Similar to a Fourier Transformation, a Wavelet Transformation consists of projecting an input signal onto the transformation basis at a given frequency. Unlike the Fourier Transformation, a Wavelet Transformation is localized in time, therefore a frequency specific wavelet is translated over functional time in order to capture the entire input signal. To do this, we start with a chosen Mother Wavelet, which can be real or complex valued, then shift it in functional time while also dilating it for a different pseudo frequency response. Let $x(t)$ be a real values input signal we wish to transform. Let $\psi(t)$ be a Mother Wavelet of our choice. For a given scale parameter $a > 0$ and translation parameter $b \in \mathbb{R}$, the resulting augmented Daughter Wavelet, $\psi(\frac{t-b}{a})$, is used to transform the input signal. The transformation is as follows:

$$W(a,b) = \frac{1}{\sqrt{a}} \int_{-\infty}^{\infty} x(t)\overline{\psi}(\tfrac{t-b}{a})dt$$

where $W(a,b)$ is the coefficient of the transformation and has the same value type of $\psi(t)$. By selecting a range of scales a and translation b to perform the transformation on will gives the Time Frequency Transformation (TFT) of our signal. Finally, the quantity of interest, as in typically frequency domain analyses, is the Power of the transformation rather than the coefficients, which is simply the squared magnitude, that is let $Y(a,b)$ be the wavelet power, then $Y(a,b) = |W(a,b)|^2$.

2 Data

2.1 Experimental Conditions

Under the guidance of Dr. Shafali Jeste, the UCLA Semel Institute conducted experiment on children with Autism Spectrum Disorder (ASD) and their Typically Developing (TD) counterparts to better understand the different implicit learning mechanism each groups utilizes in a visual paradigm. In their study, 34 TD and 37 ASD children ages 2-5 years old were exposed to continuous stream of six-colored shapes (pink squares, blue crosses, yellow circles, turquoise diamonds, grey triangles, and red octagons, see Fig 1.) [5]. These colored shapes were grouped in pairs of twos such that the shapes in a pair always and only appeared in the same order but the

three sets of pairs appeared with a random order throughout the experiment.

This design lead to two transition conditions and associated responses in the children. The within pair transitions could be learned as they were constant across the experiment, this was called the 'Expected' condition, and the between pair transition could not lead to any learning as the order was completely random, this was called the 'Unexpected' condition. Each of these conditions was considered a stimulus, resulting in a single ERP waveform. Comparing temporal aspects of the ERPs between conditions are hypothesized to indicate differences in implicit learning over the course of the experiment.

2.2 Data Structure

In the original experiment, ERP waveforms were collected at 124 electrodes across the scalp. However, not all regions of the brain elicit meaningful responses in a visual implicit learning paradigm therefore we choose to concentrate on 24 specific electrodes as was done in [1]; 12 in the frontal region and 12 in parietal region, placing 4 electrodes across each the left, center, and right sections of these regions. The recording device ran at 250 Hz for the 1 second stimulus exposure resulting in 250 time points per waveform. Finally, each stimulus, Expected and Unexpected, were applied over 120 trials each.

3 Method

3.1 Outline

In order to gain a dynamic understanding of the frequency and time response in this implicit learning experiment, we propose to apply a Wavelet Transformation via the Morlet Wavelet to single trial ERP waveforms. The resulting object is the Time-Frequency representation of the signal, which unlike purely time or frequency domain based analytical methods, shows the connected relationship these two components have. However, just as the original signal has a low SNR, so does the Time-Frequency representation. To combat this, we will utilize Principal Component Analysis (PCA) on a collection of these Time-Frequency surfaces in order to find the primary direction and degree of variation in the data.

When performing PCA it is important to maintain a ratio between the number waveforms to points per surface ratio, specifically we want this ration to be greater than 5:1, where ideally we are close to 10:1. In our experimental conditions, there are about 35 children per group and 24 electrode channels. As in [1], we are interested in the largest difference between Expected and Unexpected conditions, which occurred around trial 30. Therefore, we will consider three trials of interest: 20, 30, and 40. Further, to maintain a high ratio, we will similarly consider a 30 trial window around each of these points, that is to say the following trial sets: $[5, 35]$, $[15, 45]$, and $[25, 55]$. By doing this, we will have $35(\text{subjects}) \times 24(\text{electrodes}) \times 31(\text{trials}) = 26040$

waveforms for a given decomposition.

To ideally obtain a $10:1$ ratio means 2604 points per waveform can be included in a single surface. The Wavelet Transformation is completely dependent on user defined scale and translation parameters, therefore by a selective choice of these we can reach 2604 points per waveform. In this working example, ERP waveforms were sampled at 250 Hz for 1000 ms, therefore 250 time points per signal. Using all these time points, would only leave about 10 scale parameters available, therefore, if we down sample every third time points, e.g. points $1, 4, 7, \ldots$, we will then have 84 translation parameters, which leaves 31 scale parameters available. For computational reasons, these 31 frequencies will be evenly distributed between .5 Hz and 16 Hz on a $\log_2$ scale. This exactly gives the number of points per waveform exactly, $84 \times 31 = 2604$.

Finally, by performing PCA along column vectors of a given collection of Time-Frequency surfaces, we can extract first principal component vectors and values which can be combined to form a principal power surface. By doing this separately for each trial window, condition, and group, we will be able to examine longitudinal differences between experimental conditions and compare these differences between the TD and ASD groups.

3.2 Notation

Let $X_{ijk\ell}(t)$ represent the micro-voltage of the ERP from subject i, at electrode j, on trial k, for condition ℓ, and at observed time t, where $i = 1, \ldots, N_g$, $j = 1. \ldots, 24$,

$k \in K_b$, $\ell = 1, 2$, and $t = -100, -96, \ldots, 900$. Further, $g = 1, 2$ therefore $N_1 = 34$ for the TD group and $N_2 = 37$ for the ASD group. Finally, K_b represents the trial window in which PCA will be performed where $K_1 = [5, 35]$, $K_2 = [15, 45]$, and $K_3 = [25, 55]$.

3.3 Algorithm

Apply the following algorithm

1. For fixed i, j, k, and l, considered the single ERP waveform $X_{ijkl}(t)$.

2. Determine the frequency and time parameters to consider for the Wavelet Transformation, let $A = \{a_1, \ldots, a_F\}$ and $B = \{b_1, \ldots, b_T\}$ be the sets of increasing frequencies and times respectively.

3. For each frequency/time parameter pair, apply Wavelet Transformation to $X_{ijkl}(t)$, call this $Y_{ijkl}(a_r, b_s)$ for $r = 1, \ldots, F$ and $s = 1, \ldots, T$. Vectorize the output as follows:

$$Y_{ijkl} = \{Y_{ijkl}(a_1, b_1), \ldots, Y_{ijkl}(a_1, b_T), \ldots, Y_{ijkl}(a_F, b_1), \ldots, Y_{ijkl}(a_F, b_T)\}$$

4. Repeat the above steps $i = 1, \ldots, N_g$, $j = 1, \ldots, 24$, and $k \in K_b$. Collect each vectorized output as columns in matrix Z_{blg}, for trial window b, condition ℓ, and group g.

5. Apply PCA to Z_{blg} and extract first (column) principal components. Let V^1_{gbl} and λ^1_{blg} be the first principal component vector and value respectively. We shall consider the de-vectorized the principal component vector and scale it by $\sqrt{\lambda^1_{blg}}$ to represent the first principal power surface.

6. Repeat the above steps for $b = 1, 2, 3$, and $\ell = 1, 2$, and $g = 1, 2$ separately.

4 Analysis and Results

4.1 Implementing Transformation

Before performing the Wavelet Transformation, we applied a two step filtering process to individual ERP waveforms. First, we applied a 3^{rd} order high-pass Butterworth filter at 1.25 Hz to separate the true signal from the DC shift observed in the data. This is a well known phenomenon in which the electrode system measures additional voltage around 1 Hz alongside the EEG signal due to chemical reactions between the metallic surface of the electrode and the conductive gel applied to the scalp. Second, we apply high-pass and a low-pass 3^{rd} order Butterworth filters at 4 Hz to the previously filtered signal; we do this to separate the Delta (.5 to 4 Hz) and the Theta (4 to 8 Hz) frequency bands, which are known to have clinically significant meanings in implicit learning paradigms and doing so allows for separate analyses for each band. We then implemented the algorithm described in Section 3.3 separately for each Delta and Theta signal types created.

4.2 Results

With EEG data and especially with young children, it is extremely common to get 'bad' trial in the form of closed eyes or crying for example resulting in missing data for these exposures. This caused fewer than expected waveforms to be included in the various PCA decompositions, reducing the idealized $10:1$ ration of waveforms to points per surface. The actual ratios ranged from $5.03:1$ to $7.9:1$, while which may be smaller than the ideal ration still meet the recommended $5:1$ ratio.

In order to ensure the comparability between trials and conditions within groups and frequency bands, we look for a similar direction of variation in the unit length first principal component vector. Figures 2 and 3 show the de-vectorized leading eigenvectors across trials and conditions for Delta and Theta frequencies respectively in the ASD group. Figures 4 and 5 show the same for the TD group. In each figure, we see that both across trials and conditions the direction of variation, that is the surface itself, is nearly uniform. This suggests that PCA extracted the same underlying structure for each group/frequency pair. Therefore we are justified in comparing scaled versions of these surfaces, using the leading eigenvalue, to detect true longitudinal and condition differences.

As previously stated, we scale the leading eigenvector extracted from PCA using the square-root of its associated eigenvalue; this transforms component so that it is representative of the original wavelet power that went into the decomposition,

call this the principal power. To detect condition differences, we take the principal power from the Unexpected conditions and subtract it from the Expected conditions. Finally, to see the effect power differences in the Time-Frequency representation have on temporal qualities such as amplitude, we compare to time domain averaged ERPs of the same trial, condition, and channel criteria that went into the decomposition. Figures 6, 8, 10, and 12 show principal power surfaces and differences by condition over trials and then by frequency band and group, while figures 7, 9, 11, and 13 show corresponding time domain averaged signals and differences by condition and over trials and then by frequency band and group.

4.3 Findings & Discussion

By comparing condition differences between Time-Frequency and time domain representations we can see the different effects the Delta and Theta frequency bands have on the N1-P3 complex. In the Theta band figures across groups and trials, we see a clear dip and spike around 100ms and 300ms respectively, this is the N1-P3 complex which is well studied in implicit learning paradigms [1]. It is clear from the Time-Frequency plots that there is no Theta band power differences between conditions; we see neutral values across all the Expected - Unexpected power plots. This is supported in the time domain as well; between conditions, dips and peak nearly align and their differences only resemble slight random fluctuation. This suggests that while it does not account for differences in the magnitude of the response nor

longitudinal evolution, the Theta band is very influential to the overall shape of the N1-P3 response.

We can similarly compare responses in the Delta band which is where we not only see condition and group differences but also a process evolving over trials. In the TD group, it appears there is a primarily power differential driving the amplitude differences in the time domain. We see trial 30 has the greatest magnitude difference in amplitude between Expected and Unexpected conditions. In the Time-Frequency plots we see a corresponding power differential at the end of the Delta band. We observed a slightly similar results in the ASD group. There is some sort of longitudinal process occurring; we see a power differential that maximizes about trial 30 corresponding with a maximization of the amplitude difference in the time domain. Combined, these suggests that the Delta band is driving the amplitude difference in the time domain, which is maximized around trial 30, consistent with results found in [1].

This approach to ERP analysis highlights its usefulness in showing the interconnected relationship that time and frequency have. Use of Wavelet Transformations gives clear evidence regarding what frequencies are driving certain temporal responses. Only using a single of the two domains to perform analysis leaves an incomplete images of the true underlying mechanics. Time domain analysis can provide useful information regarding exact response differences to certain stimuli and frequency domain analysis gives insight to the influential frequencies underlying a signal but

through a combined Time-Frequency analysis we are able to more robustly analyze these otherwise distinct characteristics.

References

[1] Hasenstab, K. , Sugar, C. A., Telesca, D. , McEvoy, K. , Jeste, S. and Şentürk, D. (2015), Identifying longitudinal trends within EEG experiments. Biom, 71: 1090-1100. doi:10.1111/biom.12347

[2] Hernando Ombao , Moon-ho Ringo Ho, Time-dependent frequency domain principal components analysis of multichannel non-stationary signals, Computational Statistics & Data Analysis, v.50 n.9, p.2339-2360, May, 2006 doi>10.1016/j.csda.2004.12.011

[3] Edward M. Bernat, William J. Williams, William J. Gehring, Decomposing ERP time–frequency energy using PCA, Clinical Neurophysiology, Volume 116, Issue 6, 2005, Pages 1314-1334, ISSN 1388-2457, https://doi.org/10.1016/j.clinph.2005.01.019.

[4] Jeremy Harper, Stephen M. Malone, Edward M. Bernat, Theta and delta band activity explain N2 and P3 ERP component activity in a go/no-go task, Clinical Neurophysiology, Volume 125, Issue 1, 2014, Pages 124-132, ISSN 1388-2457, https://doi.org/10.1016/j.clinph.2013.06.025.

[5] Jeste, S. S., Kirkham, N. , Senturk, D. , Hasenstab, K. , Sugar, C. , Kupelian, C. , Baker, E. , Sanders, A. J., Shimizu, C. , Norona, A. , Paparella, T. , Freeman, S. F. and Johnson, S. P. (2015), Electrophysiological evidence of heterogeneity

in visual statistical learning in young children with ASD. Dev Sci, 18: 90-105. doi:10.1111/desc.12188

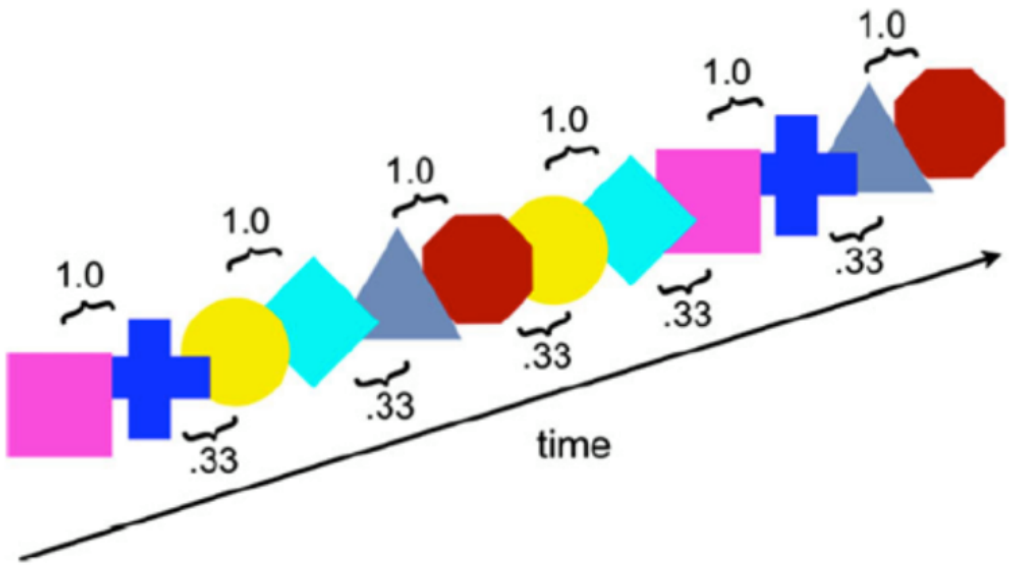

Figure 1: Depiction of the visual stimuli given to children. The Expected condition is the within pair transition that occurred with probability 1 and could be learned. The Unexpected condition is from the between pair transition that occurred randomly with probability .33 and could not be learned. [5]

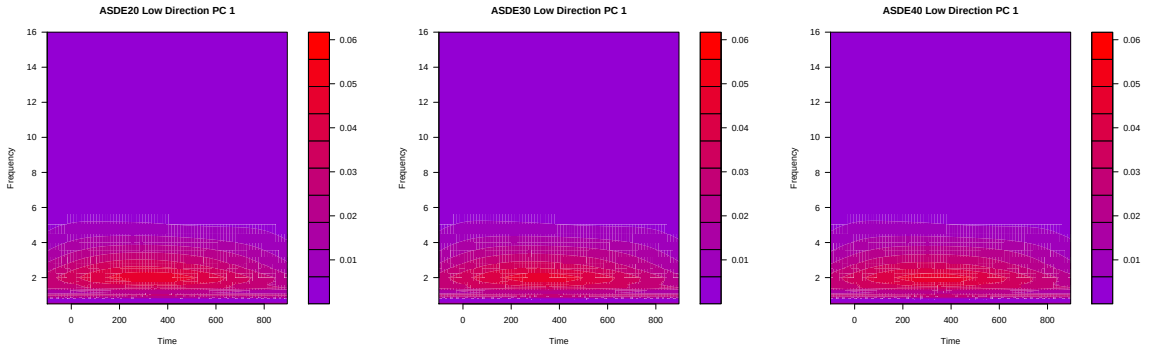

(a) (b) (c)

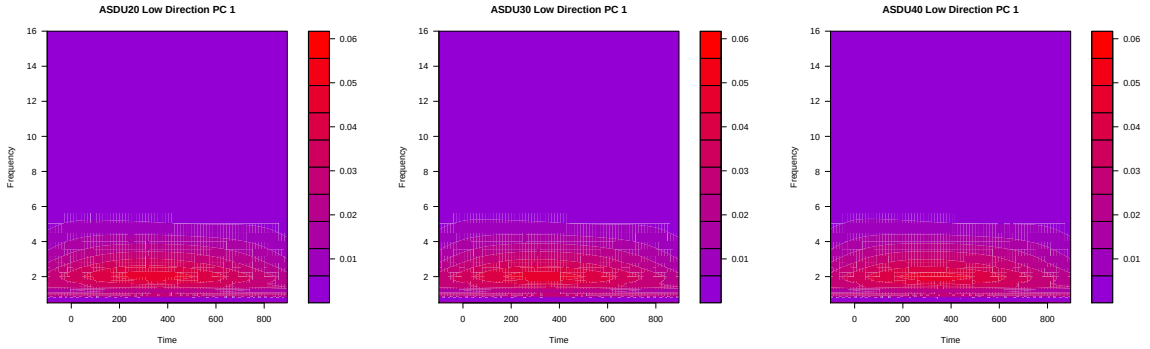

(d) (e) (f)

Figure 2: Leading principal component direction for ASD Delta frequency band. First row, (a)-(c) represent Expected condition for trials 20, 30, and 40 respectively. Second row, (d)-(f) represent Unexpected condition for trials 20, 30, and 40 respectively.

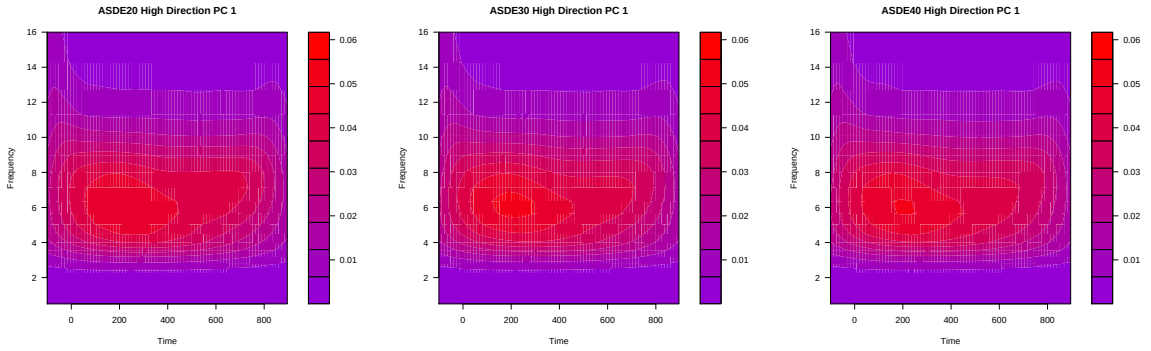

(a) (b) (c)

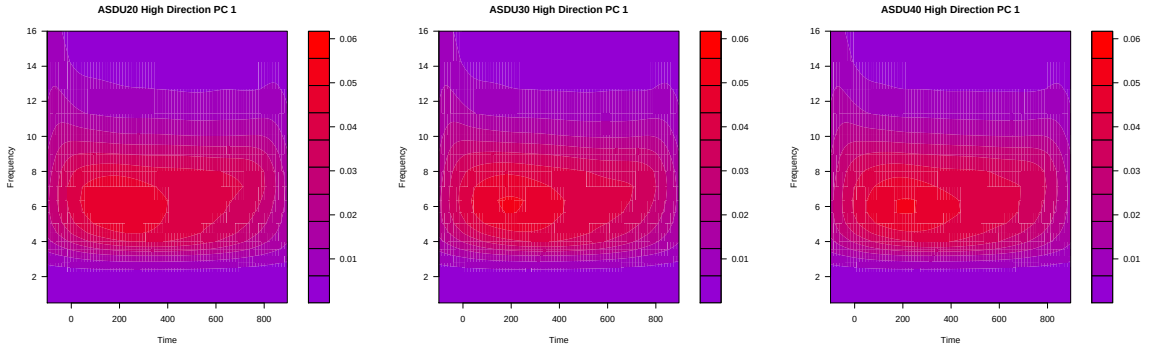

(d) (e) (g)

Figure 3: Leading principal component direction for ASD Theta frequency band. First row, (a)-(c) represent Expected condition for trials 20, 30, and 40 respectively. Second row, (d)-(f) represent Unexpected condition for trials 20, 30, and 40 respectively.

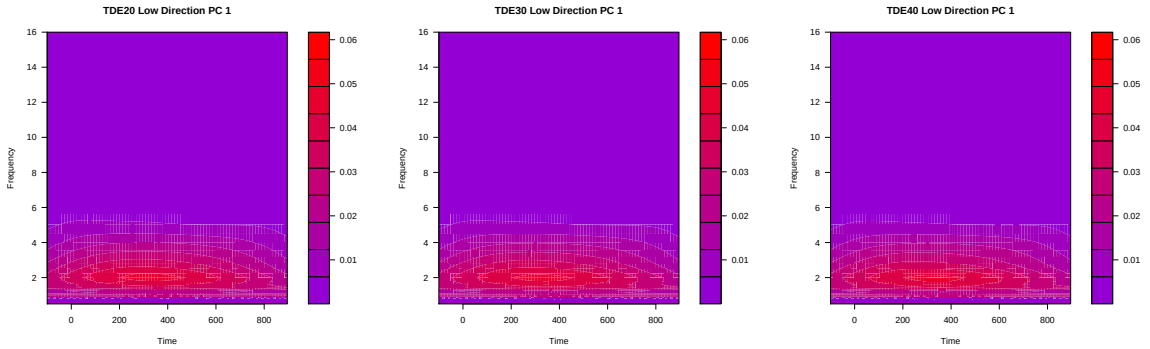

(a) (b) (c)

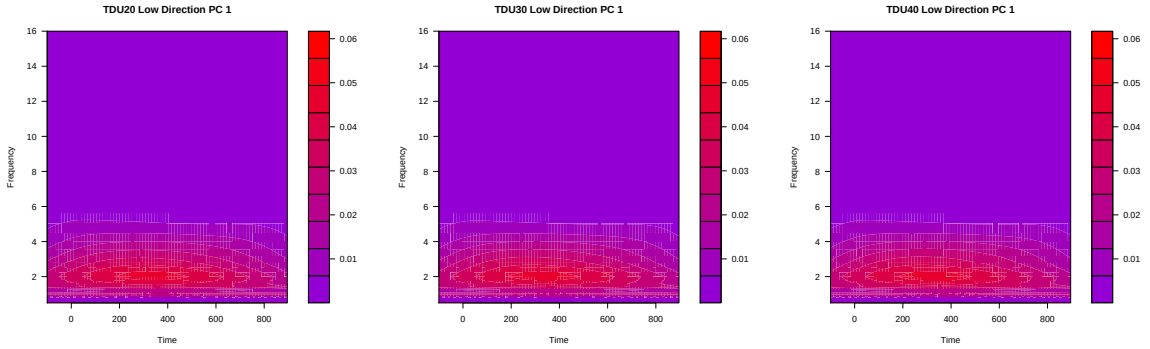

(d) (e) (f)

Figure 4: Leading principal component direction for TD Delta frequency band. First row, (a)-(c) represent Expected condition for trials 20, 30, and 40 respectively. Second row, (d)-(f) represent Unexpected condition for trials 20, 30, and 40 respectively.

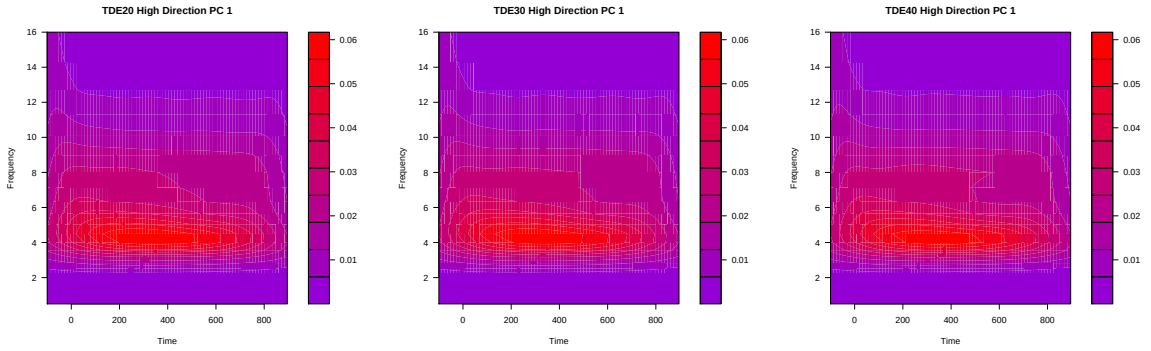

(a) (b) (c)

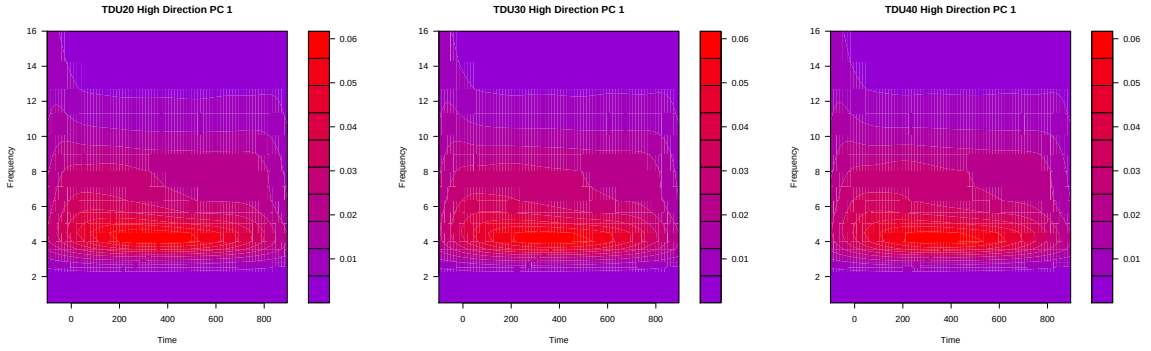

(d) (e) (f)

Figure 5: Leading principal component direction for TD Theta frequency band. First row, (a)-(c) represent Expected condition for trials 20, 30, and 40 respectively. Second row, (d)-(f) represent Unexpected condition for trials 20, 30, and 40 respectively.

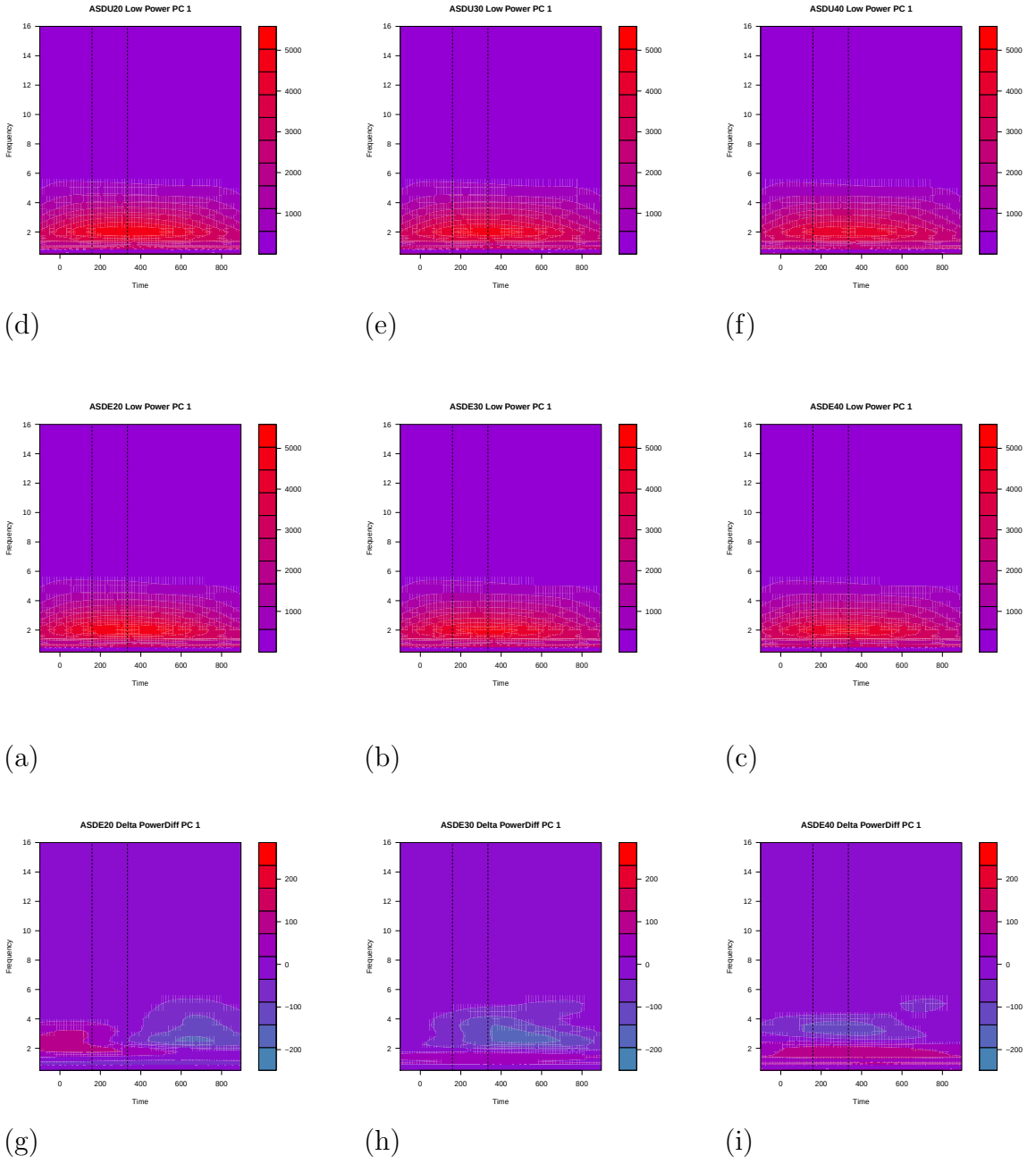

Figure 6: Leading principal component power for ASD Delta frequency band with differences. First row, (a)-(c) represent Expected condition for trials 20, 30, and 40 respectively. Second row, (d)-(f) represent Unexpected condition for trials 20, 30, and 40 respectively. Third row, (g)-(i) represent (Expected - Unexpected) for trials 20, 30, and 40.

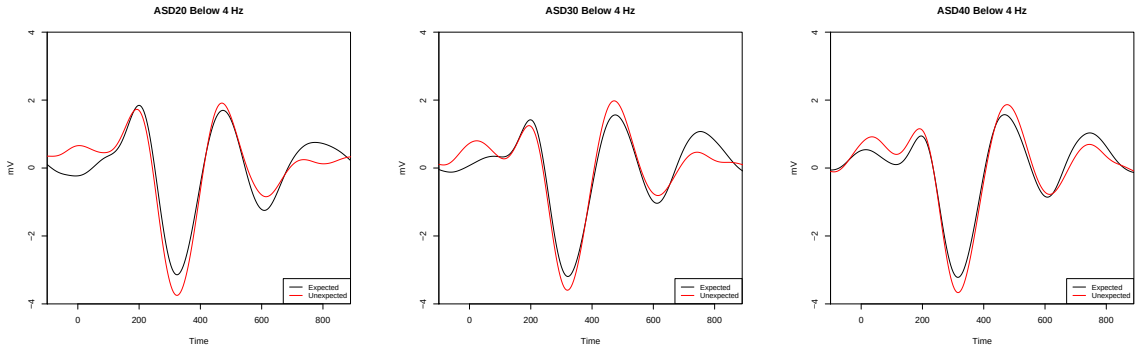

(a) (b) (c)

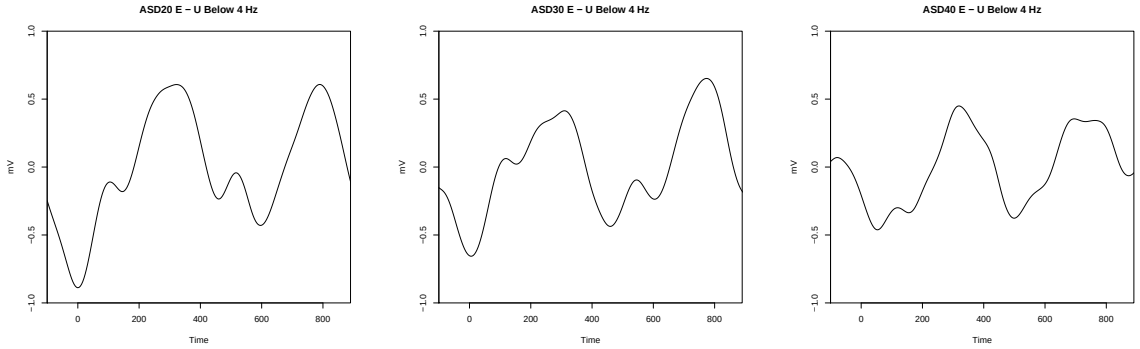

(d) (e) (f)

Figure 7: Time averaged ERPs with same inclusion criteria as previous figure for ASD Delta frequency band with differences. First row, (a)-(c) represent Expected (black) and Unexpected (red) conditions for trials 20, 30, and 40 respectively. Second row, (d)-(f) (Expected - Unexpected) waveform for trials 20, 30, and 40.

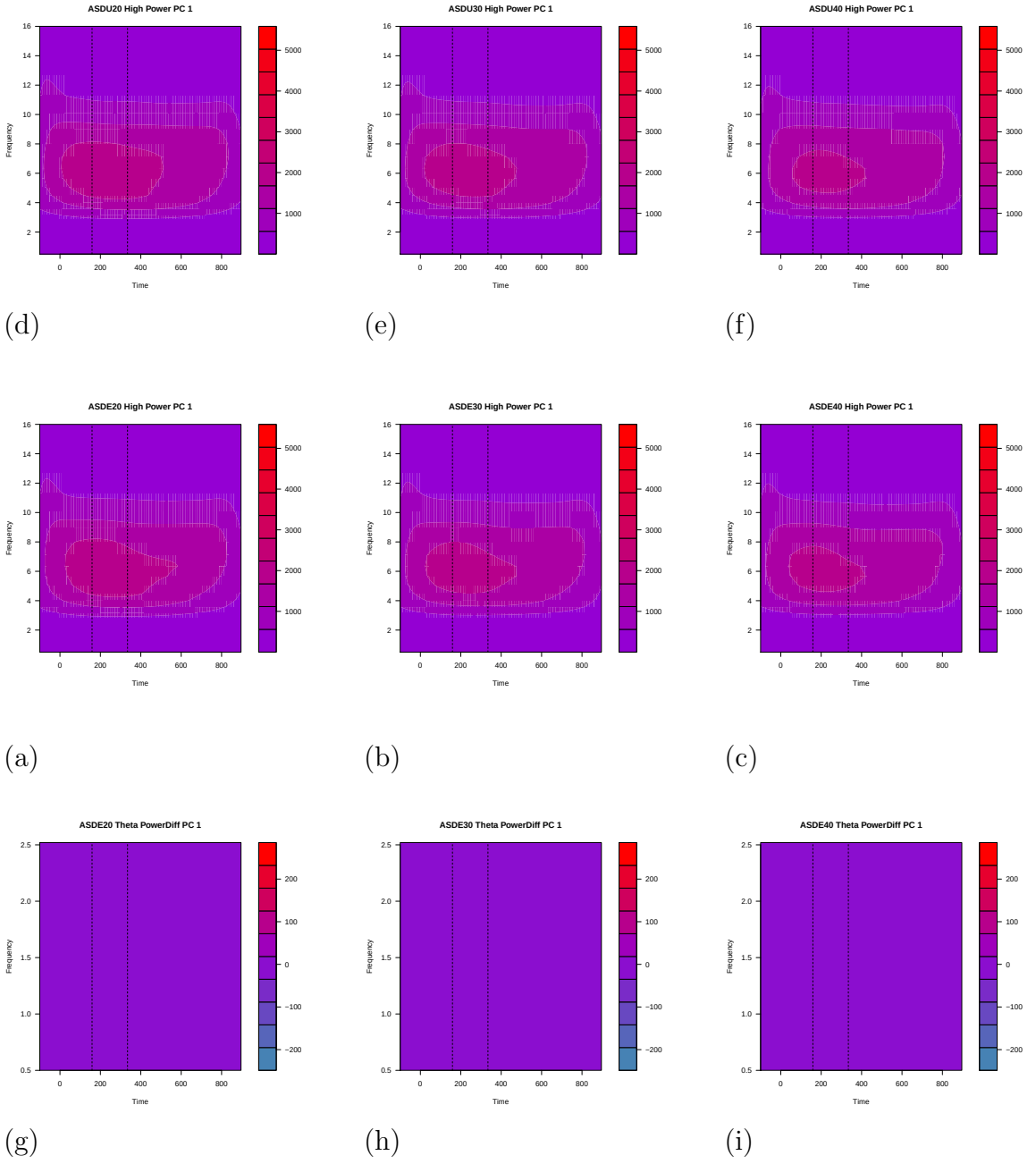

(d) (e) (f)

(a) (b) (c)

(g) (h) (i)

Figure 8: Leading principal component power for ASD Theta frequency band with differences. First row, (a)-(c) represent Expected condition for trials 20, 30, and 40 respectively. Second row, (d)-(f) represent Unexpected condition for trials 20, 30, and 40 respectively. Third row, (g)-(i) represent (Expected - Unexpected) for trials 20, 30, and 40.

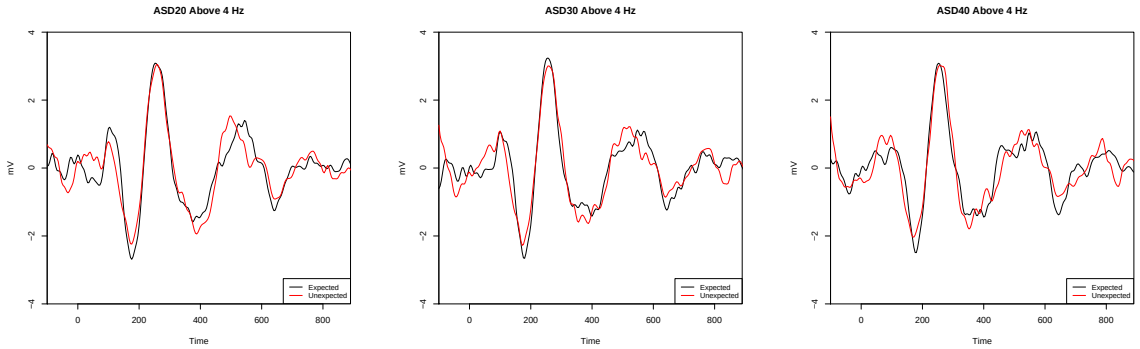

(a) (b) (c)

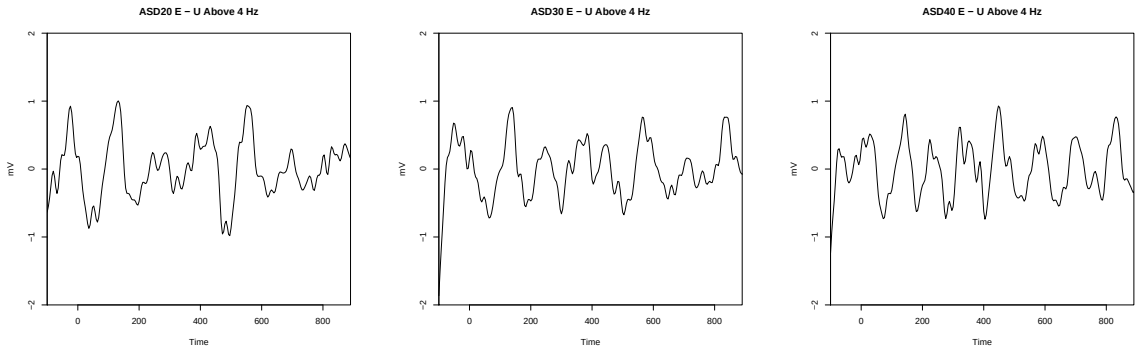

(d) (e) (f)

Figure 9: Time averaged ERPs with same inclusion criteria as previous figure for ASD Theta frequency band with differences. First row, (a)-(c) represent Expected (black) and Unexpected (red) conditions for trials 20, 30, and 40 respectively. Second row, (d)-(f) (Expected - Unexpected) waveform for trials 20, 30, and 40.

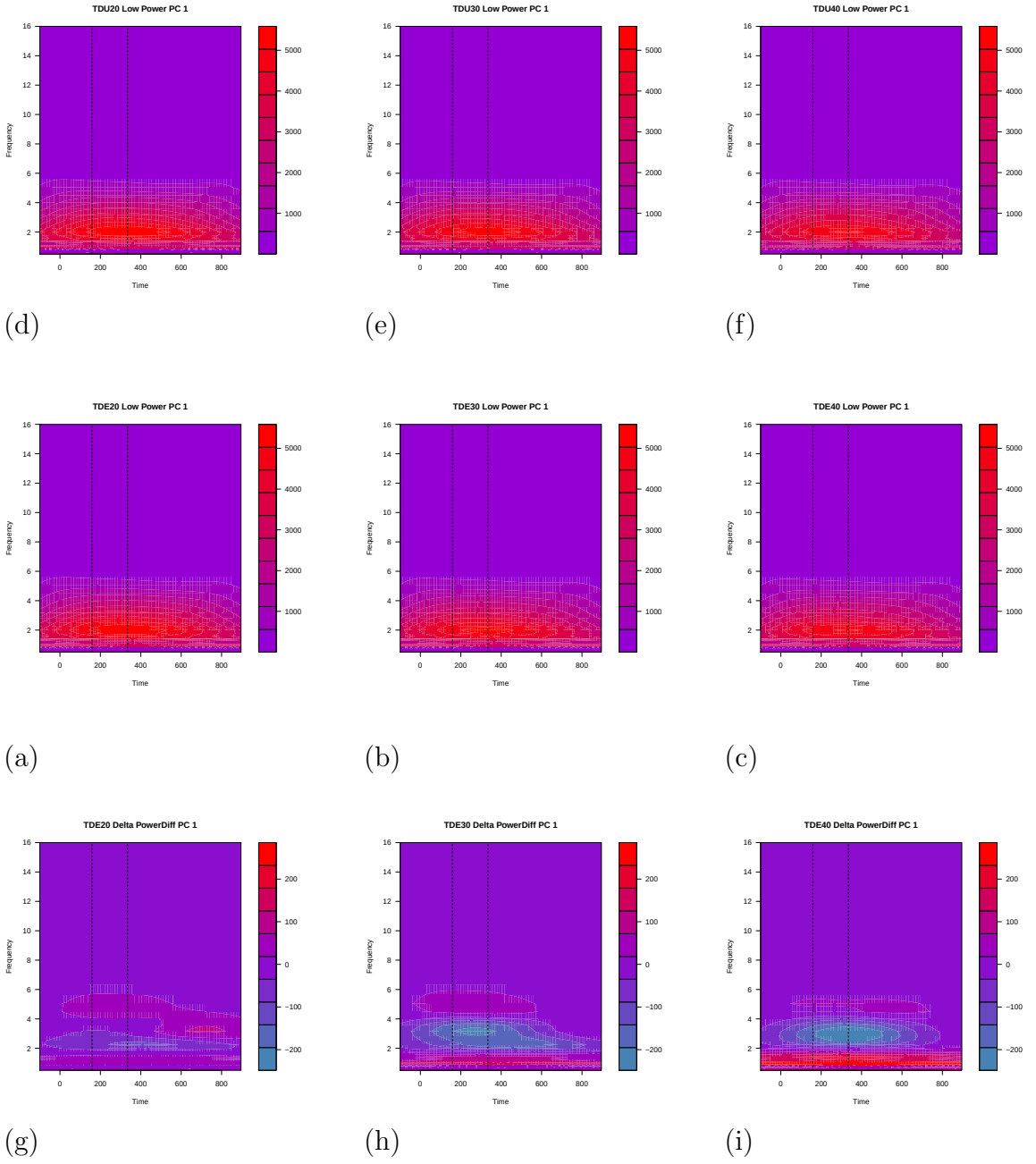

Figure 10: Leading principal component power for TD Delta frequency band with differences. First row, (a)-(c) represent Expected condition for trials 20, 30, and 40 respectively. Second row, (d)-(f) represent Unexpected condition for trials 20, 30, and 40 respectively. Third row, (g)-(i) represent (Expected - Unexpected) for trials 20, 30, and 40.

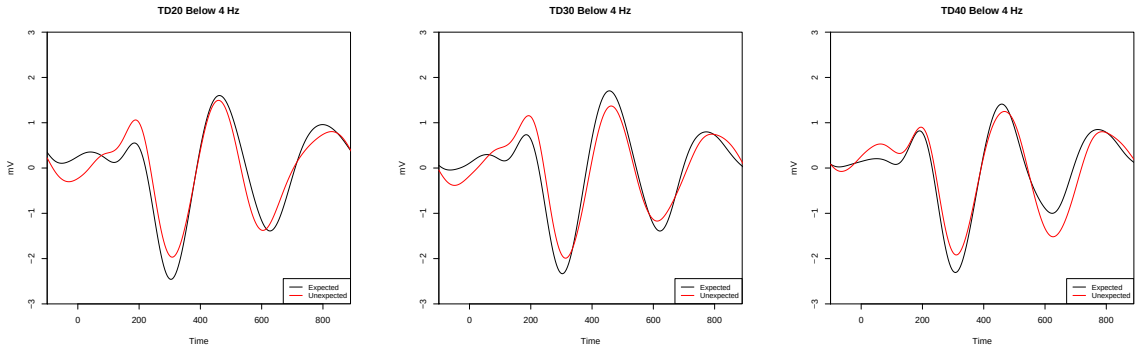

(a) (b) (c)

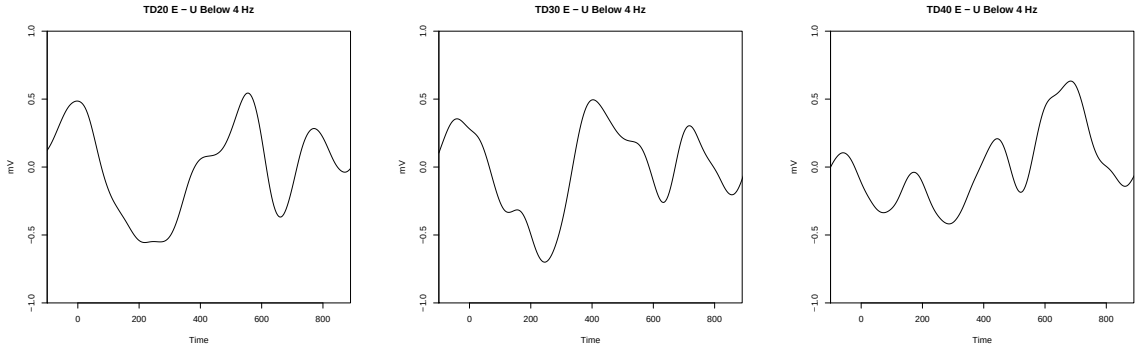

(d) (e) (f)

Figure 11: Time averaged ERPs with same inclusion criteria as previous figure for TD Delta frequency band with differences. First row, (a)-(c) represent Expected (black) and Unexpected (red) conditions for trials 20, 30, and 40 respectively. Second row, (d)-(f) (Expected - Unexpected) waveform for trials 20, 30, and 40.

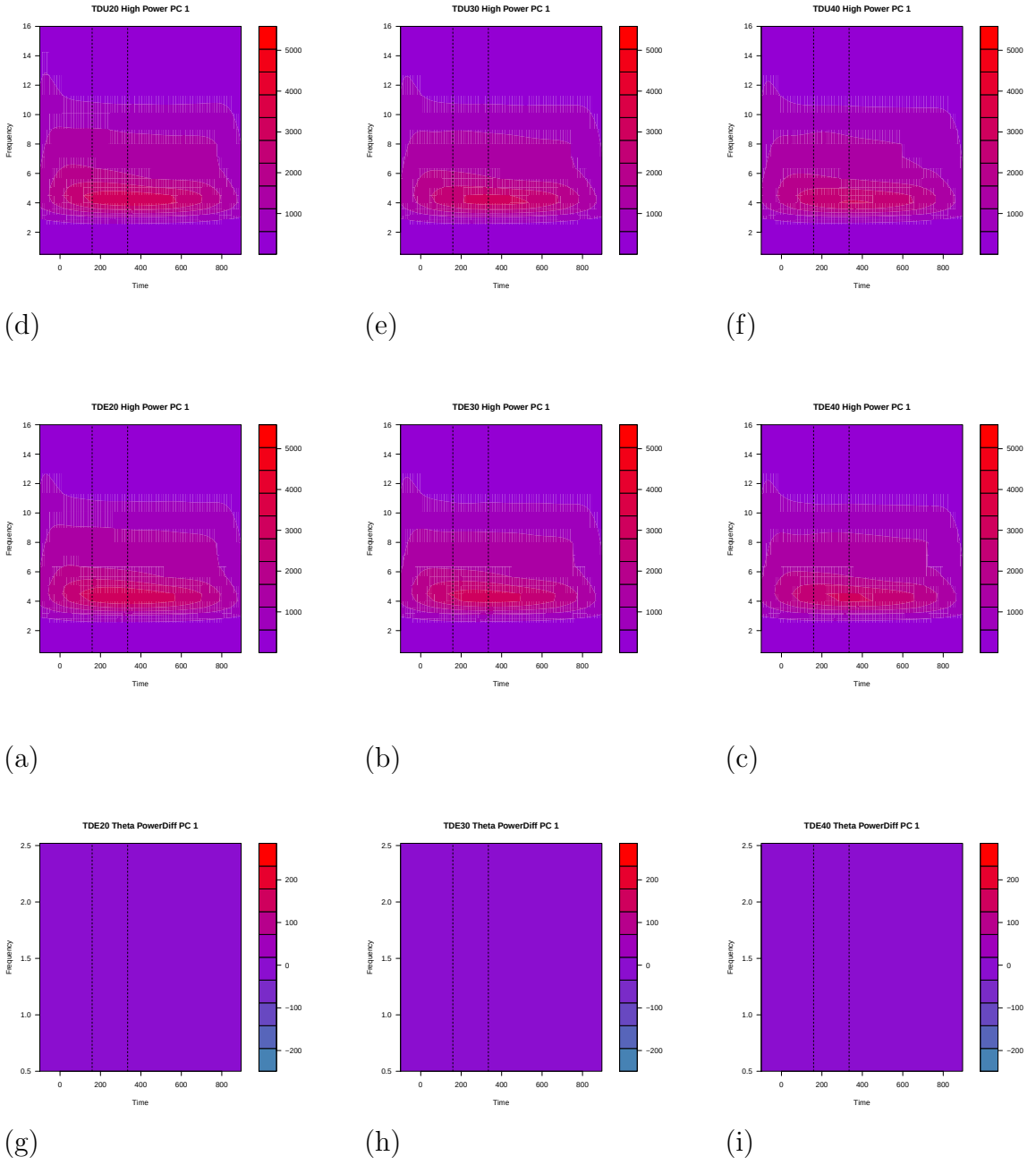

(d) (e) (f)

(a) (b) (c)

(g) (h) (i)

Figure 12: Leading principal component power for TD Theta frequency band with differences. First row, (a)-(c) represent Expected condition for trials 20, 30, and 40 respectively. Second row, (d)-(f) represent Unexpected condition for trials 20, 30, and 40 respectively. Third row, (g)-(i) represent (Expected - Unexpected) for trials 20, 30, and 40.

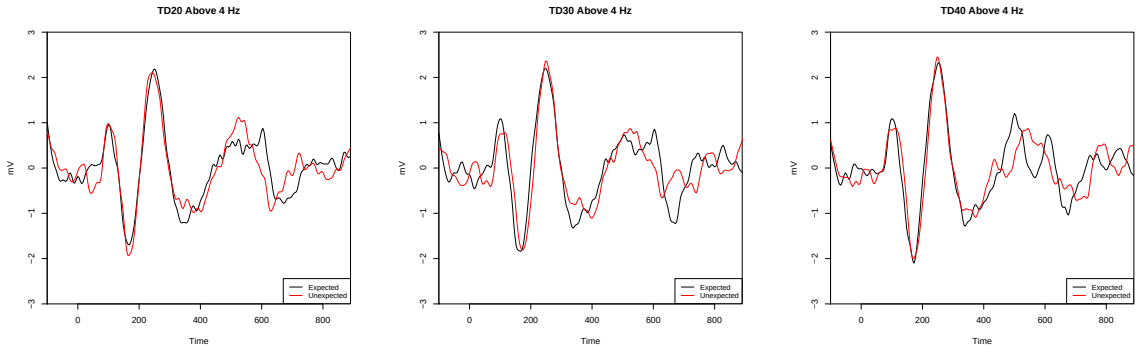

(a) (b) (c)

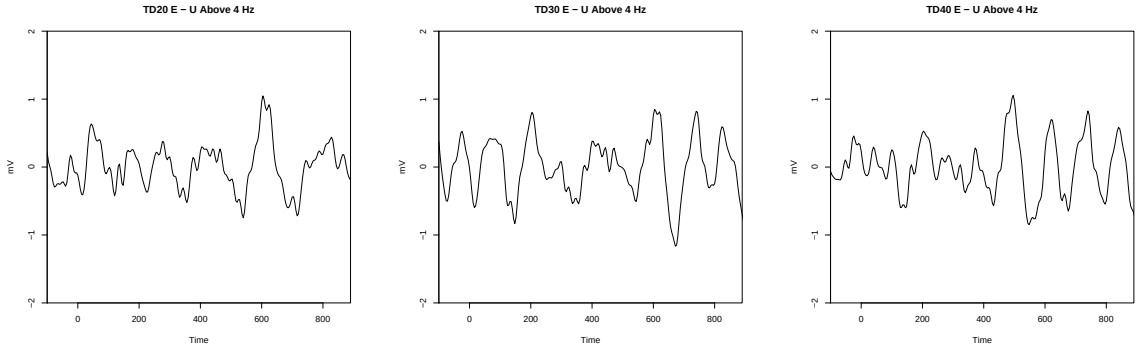

(d) (e) (f)

Figure 13: Time averaged ERPs with same inclusion criteria as previous figure for TD Theta frequency band with differences. First row, (a)-(c) represent Expected (black) and Unexpected (red) conditions for trials 20, 30, and 40 respectively. Second row, (d)-(f) (Expected - Unexpected) waveform for trials 20, 30, and 40.